Hypothalamic prolyl endopeptidase (PREP) regulates pancreatic insulin and glucagon secretion in mice

Jung Dae Kim[a,b], Chitoku Toda[a,b], Giuseppe D'Agostino[a,b,1], Caroline J. Zeiss[c], Ralph J. DiLeone[d], John D. Elsworth[d], Richard G. Kibbey[e,f], Owen Chan[e], Brandon K. Harvey[g], Christopher T. Richie[g], Mari Savolainen[g,h], Timo Myöhänen[h], Jin Kwon Jeong[a,b], and Sabrina Diano[a,b,c,i,2]

Departments of [a]Obstetrics, Gynecology, and Reproductive Sciences, [d]Psychiatry, [e]Internal Medicine, [f]Cellular and Molecular Physiology, [i]Neurobiology, [b]Program in Integrative Cell Signaling and Neurobiology of Metabolism, [c]Section of Comparative Medicine, Yale University School of Medicine, New Haven, CT 06520; [g]Intramural Research Program, National Institute on Drug Abuse, Baltimore, MD 21224; and [h]Faculty of Pharmacy, University of Helsinki, 00014, Helsinki, Finland

Edited* by Jeffrey M. Friedman, The Rockefeller University, New York, NY, and approved June 30, 2014 (received for review April 3, 2014)

Prolyl endopeptidase (PREP) has been implicated in neuronal functions. Here we report that hypothalamic PREP is predominantly expressed in the ventromedial nucleus (VMH), where it regulates glucose-induced neuronal activation. PREP knockdown mice (*Prep*$^{gt/gt}$) exhibited glucose intolerance, decreased fasting insulin, increased fasting glucagon levels, and reduced glucose-induced insulin secretion compared with wild-type controls. Consistent with this, central infusion of a specific PREP inhibitor, S17092, impaired glucose tolerance and decreased insulin levels in wild-type mice. Arguing further for a central mode of action of PREP, isolated pancreatic islets showed no difference in glucose-induced insulin release between *Prep*$^{gt/gt}$ and wild-type mice. Furthermore, hyperinsulinemic euglycemic clamp studies showed no difference between *Prep*$^{gt/gt}$ and wild-type control mice. Central PREP regulation of insulin and glucagon secretion appears to be mediated by the autonomic nervous system because *Prep*$^{gt/gt}$ mice have elevated sympathetic outflow and norepinephrine levels in the pancreas, and propranolol treatment reversed glucose intolerance in these mice. Finally, re-expression of PREP by bilateral VMH injection of adeno-associated virus–PREP reversed the glucose-intolerant phenotype of the *Prep*$^{gt/gt}$ mice. Taken together, our results unmask a previously unknown player in central regulation of glucose metabolism and pancreatic function.

central glucose sensing | sympathetic nervous system | peripheral hormonal regulation

Prolyl endopeptidase (PREP; EC 3.4.21.26) is a highly conserved enzyme (1). In humans and rodents it is highly expressed in the brain (2), including the cortex, striatum, hypothalamus, hippocampus, and amygdala (3–6). The physiological role of PREP remains elusive (7). Many studies have focused on the putative effect of PREP on neuropeptide levels because this enzyme could function to cleave virtually all neuropeptides shorter than 30 amino acids that contain an internal proline residue (8).

However, much of our understanding of this enzyme is based on in vitro data. Because PREP's putative targets regulate a large number of signaling pathways, PREP has the capacity to regulate a variety of cellular tasks.

To gain a better understanding of the role of PREP in the hypothalamus, we analyzed the effect of PREP knockdown on hypothalamic mechanisms including glucose and energy metabolism.

Results

Hypothalamic PREP Expression. In the central nervous system, *Prep* mRNA was found in the hypothalamus (Fig. 1*A*), hippocampus, and cortex (5, 6). Within the hypothalamus, higher expression of *Prep* mRNA was detected in the ventromedial nucleus (VMH) (Fig. 1*A* and Fig. S1*A*). In mice in which PREP was knocked down by the gene trap (*Prep*$^{gt/gt}$ mice) (9), β-gal expression showed an expression pattern similar to that seen by the in situ hybridization (Fig. 1*B* and Fig. S1*B*). *Prep* mRNA and protein expression were also observed in peripheral organs (Fig. S1 *C* and *D*). A significant decrease of PREP protein levels was found in all examined tissues of *Prep*$^{gt/gt}$ mice, including the VMH (Fig. S1*E*). Analysis of the mRNA expression levels of two other serine proteases, dipeptidyl peptidase-4 and acylamino acid-releasing enzyme, in the hypothalamus and peripheral organs such as liver, brown adipose tissue (BAT), and pancreas showed no compensatory changes in their mRNA levels in *Prep*$^{gt/gt}$ mice compared with their WT controls (Fig. S2, *Upper* and *Lower*).

Metabolic Characterization of *Prep*$^{gt/gt}$ Mice. Prep gene-trap (*Prep*$^{gt/gt}$) mice fed on a standard chow diet showed no difference in body weights and body composition compared with their WT controls (Fig. S3 *A* and *B*). Further analysis of food and water intake did not reveal any difference. (Fig. S3 *C* and *D*).

Impaired Glucose Metabolism in *Prep*$^{gt/gt}$ Mice. The VMH is considered an important center for glucose regulation (for review see ref. 10). *Prep*$^{gt/gt}$ mice had increased fasting blood glucose levels compared with their WT controls (time 0 in Fig. 1*C*). A glucose tolerance test (GTT) showed that *Prep*$^{gt/gt}$ mice had a marked increase in blood glucose levels compared with WTs (Fig. 1*C*). During GTT, significant lower insulin levels were found in *Prep*$^{gt/gt}$ mice compared with WT controls (Fig. 1*D*). On the other hand, fasting glucagon levels were elevated in *Prep*$^{gt/gt}$ mice compared with their WT controls (Fig. 1*E*). A pyruvate tolerance test (PTT) showed that *Prep*$^{gt/gt}$ mice had an enhanced glucose production (Fig. 1*F*) that was associated with increased mRNA expression of liver enzymes involved in gluconeogenesis

Significance

The ventromedial nucleus of the hypothalamus (VMH) plays an important role in the regulation of glucose metabolism. Here we show that prolyl endopeptidase (PREP), a serine protease, is expressed in the VMH where it functions to regulate glucose-induced insulin secretion. Experimental knockdown of central PREP induced impairment of VMH glucose sensing, resulting in reduced insulin and increased glucagon secretion by the pancreas via altered sympathetic outflow. Our data reveal PREP as a new hypothalamic player in the control of glucose homeostasis.

Author contributions: S.D. designed research; J.D.K., C.T., G.D., C.J.Z., J.D.E., R.G.K., O.C., M.S., J.K.J., and S.D. performed research; R.J.D., J.D.E., B.K.H., C.T.R., M.S., and T.M. contributed new reagents/analytic tools; J.D.K., C.T., G.D., C.J.Z., R.G.K., O.C., J.K.J., and S.D. analyzed data; and J.D.K. and S.D. wrote the paper.

The authors declare no conflict of interest.

*This Direct Submission article had a prearranged editor.

[1]Present address: Rowett Research Institute, University of Aberdeen, Aberdeen AB21 9SB, United Kingdom.

[2]To whom correspondence should be addressed. Email: sabrina.diano@yale.edu.

This article contains supporting information online at www.pnas.org/lookup/suppl/doi:10.1073/pnas.1406000111/-/DCSupplemental.

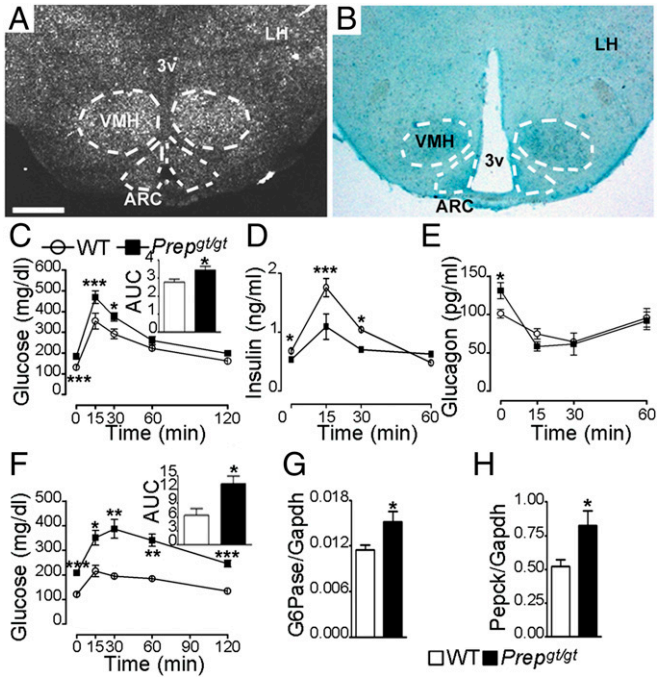

Fig. 1. (*A* and *B*) VMH PREP and glucose metabolism. Light microscopic photograph of representative coronal sections after in situ hybridization (*A*) or LacZ staining (*B*). (*C*) Results from the GTT in *Prep*$^{gt/gt}$ and WT. The area AUC analysis showed a significant glucose intolerance in *Prep*$^{gt/gt}$ mice compared with the WT controls (n = 10 for each group). (*D*) Circulating insulin levels in WT (n = 6) and *Prep*$^{gt/gt}$ mice (n = 4) during the GTT. (*E*) Glucagon levels during GTT (WT: n = 6; *Prep*$^{gt/gt}$: n = 4). (*F*) The results of PTT in *Prep*$^{gt/gt}$ and WT mice (n = 4/group). (*G* and *H*) Increased G6pase and Pepck mRNA expression in the *Prep*$^{gt/gt}$ mice (n = 6) compared with their WT controls (n = 6). All data represent the mean ± SEM. *P < 0.05; **P < 0.01; ***P < 0.001. [Scale bar in *A* (also applies to *B*), 2 mm.] ARC, arcuate nucleus; LH, lateral hypothalamus; 3v, third ventricle; VMH, ventromedial nucleus.

such as glucose-6-phosphatase (G6Pase) and phosphoenolpyruvate carboxykinase (Pck1) (Fig. 1 *G* and *H*).

Glucose Responsiveness of VMH Neurons Is Impaired in *Prep*$^{gt/gt}$ Mice. To determine the effect of glucose on VMH neuronal activation, we assessed the effect of peripheral glucose administration on c-fos staining in WT and *Prep*$^{gt/gt}$ mice (Fig. 2 *A*–*C*). Glucose administration to WT mice induced a significant increase of c-fos immunolabeling in the VMH compared with baseline WT saline-treated mice (Fig. 2 *A* and *C*; 210.00 ± 17.41%). However, glucose injection of *Prep*$^{gt/gt}$ mice induced a significantly smaller increase in c-fos immunoreactivity (Fig. 2 *B* and *C*; 138.80 ± 5.13%; P < 0.05), suggesting that *Prep*$^{gt/gt}$ mice have impaired glucose sensitivity in the VMH. No difference in c-fos staining was found in the hypothalamic arcuate (Fig. S4*A*) and dorsomedial nuclei (Fig. S4*B*).

Decreased Glucose-Induced Insulin Receptor Phosphorylation in the Hypothalamus of *Prep*$^{gt/gt}$ Mice. Because reduction in the activation of insulin receptors in the VMH induced glucose intolerance in the absence of weight gain (11), we analyzed insulin receptor (IR) phosphorylation levels in fed and fasted states and 5 min after the systemic saline or glucose administration. In WT mice, feeding induced a significant increase in the phosphorylated-insulin receptor (pIR)/insulin receptor (IR) ratio in the VMH compared to fasting (Fig. 2*D*). Although in *Prep*$^{gt/gt}$ mice feeding also induced a significant increase of the pIR/IR ratio in the VMH, this increase was significantly lower than that of WT mice (Fig. 2*D*). Similarly, 5-min glucose-treated fasted WT and *Prep*$^{gt/gt}$ mice showed significant increases in the pIR/IR ratio of the VMH compared with their saline-treated fasted control (Fig. 2*E*). However, the increase in the *Prep*$^{gt/gt}$ mice was significantly lower than that of WT (Fig. 2*E*), suggesting impairment in

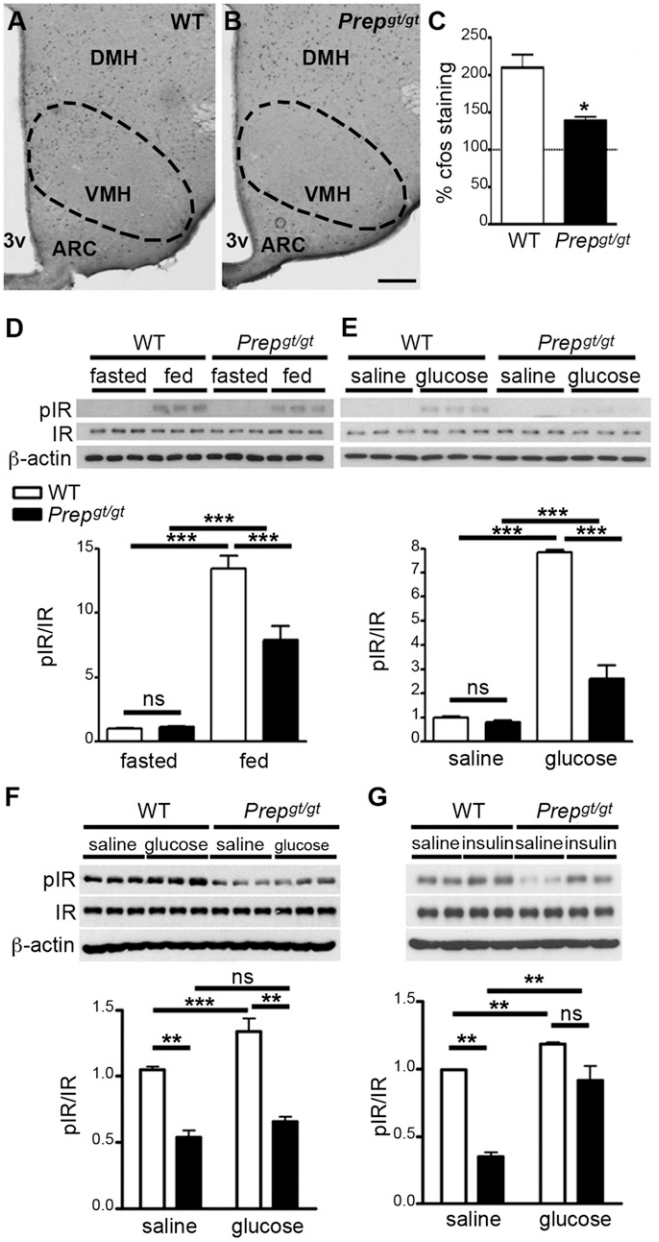

Fig. 2. PREP effect on glucose-induced VMH neuronal and insulin receptor activation. (*A* and *B*) Representative microphotographs showing c-fos immunolabeling in the hypothalami of a WT (*A*) and a *Prep*$^{gt/gt}$ mouse (*B*) injected with glucose. (*C*) Results of the quantification of c-fos immunolabeling in the medial VMH of WT and *Prep*$^{gt/gt}$ mice injected with glucose (n = 3 per group). Data are expressed as percentage of WT mice treated with saline. (*D* and *E*) Western blot images and graphs showing the analysis of phosphorylated and total insulin receptor (pIR and IR, respectively) and β-actin in the VMH of fed and fasted WT and *Prep*$^{gt/gt}$ mice (*A*: n = 3/group) and in the VMH of fasted WT and *Prep*$^{gt/gt}$ mice 5 min after either saline or glucose administration (*B*: n = 3/group). (*F*) pIR/IR ratio in the hypothalamus of fed *Prep*$^{gt/gt}$ mice (n = 3) compared with fed WT controls (n = 3) after saline or glucose administration. (*G*) pIR/IR ratio in the hypothalamus of fed *Prep*$^{gt/gt}$ mice compared with fed WT controls after saline or insulin administration (n = 3–4/group). All data represent the mean ± SEM. *P < 0.05; **P < 0.01; ***P < 0.001. ns, not statistically significant. [Scale bar in *B* (also applies to *A*), 100 μm.]

glucose-induced phosphorylation of insulin receptors. Although no difference in pIR/IR ratio was found in the VMH of fasted WT compared with fasted *Prep*$^{gt/gt}$ (Fig. 2 *D* and *E*), in the fed state *Prep*$^{gt/gt}$ mice showed a significant lower pIR/IR ratio in the hypothalamus compared with fed WT controls ($P < 0.01$; Fig. 2*F*). Glucose administration to fed WT mice significantly increased the pIR/IR ratio (Fig. 2*F*), which was absent in fed *Prep*$^{gt/gt}$ mice (Fig. 2*F*). In contrast to glucose, systemic insulin injection efficiently induced the phosphorylation of IR in fed *Prep*$^{gt/gt}$ mice (Fig. 2*G*) to a level that was not significantly different from that of fed WT controls (Fig. 2*G*).

***Prep*$^{gt/gt}$ Mice Have Normal Glucose Uptake.** An insulin tolerance test (ITT) showed similar insulin sensitivity between WT and *Prep*$^{gt/gt}$ mice (Fig. 3*A*). Consistent with this, during the hyperinsulinemic-euglycemic clamps (Fig. 3*B*; circulating insulin levels: 1.87 ± 0.28 ng/mL in WT and 1.72 ± 1.18 ng/mL in *Prep*$^{gt/gt}$ mice; $P = 0.68$), *Prep*$^{gt/gt}$ mice required similar exogenous glucose infusions to maintain euglycemia (24.44 ± 1.82 mg/kg/min in WT mice vs. 20.83 ± 3.31 mg/kg/min in *Prep*$^{gt/gt}$ mice; $P = 0.32$; Fig. 3*C*). Furthermore, whole-body glucose uptake was not significantly different between WT and *Prep*$^{gt/gt}$ mice ($P = 0.81$; Fig. 3*D*), indicating a normal insulin sensitivity of *Prep*$^{gt/gt}$ mice. Baseline hepatic glucose production was significantly increased in *Prep*$^{gt/gt}$ mice compared with WT controls (Fig. 3*E*). However, during the clamp, hepatic glucose production significantly decreased in *Prep*$^{gt/gt}$ mice, reaching a level no significantly different from that of WT controls (Fig. 3*E*), showing that the hepatic insulin resistance seen at baseline condition disappeared after insulin infusion in *Prep*$^{gt/gt}$ mice. Finally, plasma glucagon levels during clamp were measured to assess whether differences in glucagon secretion could have an indirect impact on peripheral insulin sensitivity. No differences in glucagon levels were observed between WT controls and *Prep*$^{gt/gt}$ mice (24.00 ± 1.47 pg/mL; $n = 5$ WT and 26.40 ± 4.16 pg/mL; $n = 3$ *Prep*$^{gt/gt}$ mice; $P = 0.53$), suggesting that insulin infusion strongly suppressed glucagon secretion in both experimental groups.

Intact Pancreatic Islet Function in *Prep*$^{gt/gt}$ Mice. Because PREP is also expressed in the pancreas (Fig. S1 *A* and *B*), we next assessed islets morphology and function (Fig. 3 *F*–*I*). No differences in islet staining for either insulin or glucagon were observed (Fig. 3*F*). Analysis of the density of the islets (Fig. 3*G*; $P = 0.54$) and the ratio of the area of the islets to the area of the pancreas (Fig. 3*H*; $P = 0.105$) showed no difference between the two groups. We then assessed glucose-stimulated insulin secretion (GSIS) in isolated pancreatic islets. No difference in GSIS was observed between WT and *Prep*$^{gt/gt}$ mice (Fig. 3*I*). These results indicate that *Prep*$^{gt/gt}$ mice have functionally intact pancreatic islets.

Enhanced Uncoupling Protein 1 Expression in *Prep*$^{gt/gt}$ Mice. The secretory activity of pancreatic islet cells is in part controlled by the autonomic nervous system (ANS) (12). Thus, we analyzed Enhanced Uncoupling Protein 1 (UCP1) mRNA expression in the BAT of WT and *Prep*$^{gt/gt}$ mice (13, 14). A significant increase of UCP1 mRNA levels was observed in *Prep*$^{gt/gt}$ mice ($P = 0.009$; Fig. 4*A*), whereas no differences in circulating free T4 (2.15 ± 0.11 ng/dL in $n = 14$ WT and 2.14 ± 0.12 ng/dL in $n = 11$ *Prep*$^{gt/gt}$ mice) and free T3 levels (3.52 ± 0.34 in $n = 12$ WT and 4.34 ± 0.38 in $n = 11$ *Prep*$^{gt/gt}$) were observed, suggesting that the sympathetic tone is increased in *Prep*$^{gt/gt}$ mice compared with WT mice. In support of this, when norepinephrine levels (NE) were measured in the pancreas of fasted WT and *Prep*$^{gt/gt}$ mice, significantly greater NE levels were found in fasted *Prep*$^{gt/gt}$ mice compared with fasted WT (Fig. 4*B*; $P < 0.05$). We then treated *Prep*$^{gt/gt}$ mice with Propranolol, an antagonist for β-adrenergic receptors, for 3 d with a dose that did not affect the glucose tolerance of WT controls (Fig. 4 *C* and *D*). This intervention significantly improved the GTT of *Prep*$^{gt/gt}$ mice (Fig. 4 *C* and *D*).

Effect of Central Infusion of S17092, a PREP Inhibitor, on GTT. To determine the role of central PREP on glucose metabolism, next we infused i.c.v. a specific PREP inhibitor, S17092 (15), in WT mice and performed a GTT. Thirty minutes of infusion of S17092 in WT mice significantly increased glucose levels (Fig. 4*E*). Although WT mice treated with S17092 had a slight increase of the area under the curve (AUC) (Fig. 4*E*) compared with WT treated with saline (Fig. 4*E*), this difference was not significant. Analysis of circulating insulin levels during the GTT showed that infusion of S17092 significantly lowered insulin levels in WT mice (Fig. 4*F*).

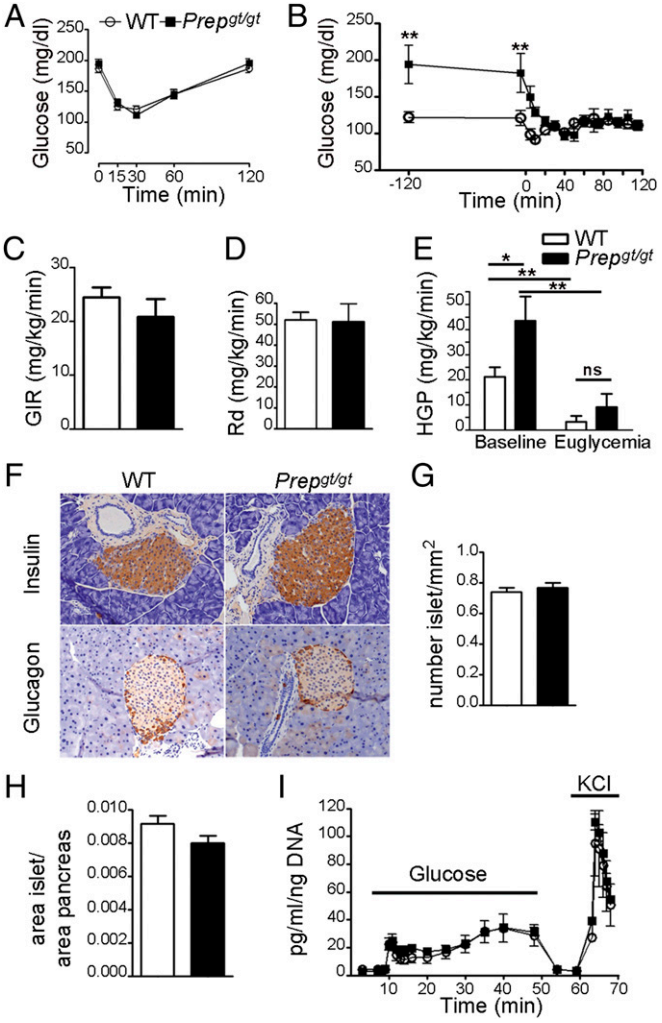

Fig. 3. PREP does not alter peripheral insulin sensitivity or ex vivo pancreatic function. (*A*) Results from the ITT showing no difference in insulin sensitivity between *Prep*$^{gt/gt}$ ($n = 8$) and WT mice ($n = 8$). (*B*) Glucose levels during a hyperinsulemic-euglycemic clamp study (WT: $n = 10$; *Prep*$^{gt/gt}$: $n = 7$). (*C*) Results showing no difference in glucose infusion rate (GIR) during a hyperinsulemic-euglycemic clamp study. (*D*) Results showing no difference in the rate of whole-body glucose disappearance (Rd) between WT ($n = 10$) and *Prep*$^{gt/gt}$ mice ($n = 7$). (*E*) Graph showing HGP in *Prep*$^{gt/gt}$ mice ($n = 7$) and their WT controls ($n = 10$) at baseline condition and during the clamp. (*F*) Representative light micrographs showing pancreatic islets stained with insulin (*Upper*) and glucagon (*Lower*) of WT and *Prep*$^{gt/gt}$ mice. (*G*) The ratio of the number of islets per square millimeter of area in WT ($n = 7$) and *Prep*$^{gt/gt}$ mice ($n = 6$). (*H*) The difference in the ratio between islet area and total pancreas area in WT ($n = 7$) and *Prep*$^{gt/gt}$ mice ($n = 6$). (*I*) Insulin secretion from isolated perifused islets in response to low and high glucose and KCl (WT: $n = 3$; *Prep*$^{gt/gt}$: $n = 3$). All data represent the mean ± SEM. *$P < 0.05$; **$P < 0.01$; ns, not statistically significant.

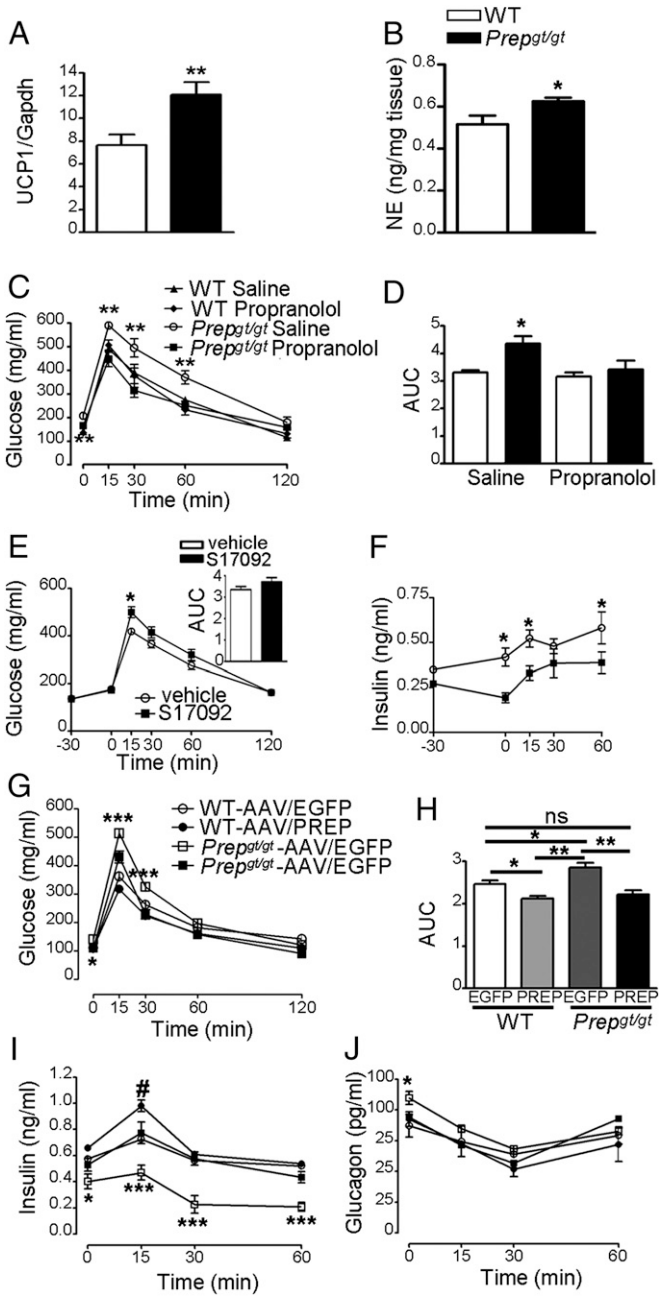

Fig. 4. VMH PREP re-expression restores glucose homeostasis. (*A*) Increase in Ucp1mRNA levels in the BAT of *Prep*$^{gt/gt}$ mice ($n = 10$) compared with their WT controls ($n = 8$). (*B*) Results from pancreas NE levels measured in fasted WT and *Prep*$^{gt/gt}$ mice ($n = 5$ per group). (*C* and *D*) GTT performed in WT ($n = 7$) and *Prep*$^{gt/gt}$ mice ($n = 7$) that were treated with saline or propranolol. The AUC in propranolol-treated *Prep*$^{gt/gt}$ mice shows a significant improvement in the GTT compared with saline-treated *Prep*$^{gt/gt}$ controls (*D*). (*E*) Results of the GTT performed in WT mice intracerebroventricularly infused for 30 min with either vehicle or S17092 ($n = 10$ for each group). Although slightly increased after S17092 treatment, analysis of the AUC showed no statistical significance between vehicle- and S17092-infused WT mice. (*F*) Circulating insulin levels in S17092-infused WT mice during a GTT ($n = 5$ for each group). (*G* and *H*) Results of a GTT in WT and *Prep*$^{gt/gt}$ mice that were infected with either AAV–EGFP or AAV–PREP ($n = 4$ for each group). (*I* and *J*) Results of insulin and glucagon measurements during GTT in WT and *Prep*$^{gt/gt}$ mice that were infected with either AAV–EGFP or AAV–PREP. All data represent the mean ± SEM. $^*P < 0.05$; $^{**}P < 0.01$; $^{***}P < 0.001$ compared the other groups. ns, not statistically significant.

Re-expression of PREP in the VMH of *Prep*$^{gt/gt}$ Mice. To assess whether re-expression of PREP in the VMH could rescue glucose intolerance and pancreatic function in *Prep*$^{gt/gt}$ mice, we cloned a cDNA encoding mouse prolyl endopeptidase into adeno-associated virus (AAV) expression vector carrying EF1α promoter and bilaterally injected in the VMH of WT and *Prep*$^{gt/gt}$ mice (Fig. S5 *A*–*C*). An AAV vector carrying EGFP was used as control (Fig. S5 *A*–*C*). Two weeks after the intracranial injections, fasting glucose levels (time 0) in *Prep*$^{gt/gt}$ mice infected with AAV–PREP (110.5 ± 4.25 mg/dL; Fig. 4*G*) were significantly lower than those of *Prep*$^{gt/gt}$ mice (140.5 ± 5.42 mg/dL; Fig. 4*G*). No significant differences in fasting glucose levels were found between WT mice infected with AAV–EGFP and *Prep*$^{gt/gt}$ mice infected with AAV–PREP (Fig. 4*G*). Furthermore, *Prep*$^{gt/gt}$ mice infected with AAV–PREP showed significantly lower glucose levels compared with controls (Fig. 4*G*). Analysis of the AUC showed that both WT and *Prep*$^{gt/gt}$ mice infected with AAV–PREP had a significantly lower AUC compared with either WT or *Prep*$^{gt/gt}$ controls (Fig. 4*H*). Circulating insulin level measurements showed a significant increase in insulin levels in treated *Prep*$^{gt/gt}$ mice compared with controls (Fig. 4*I*). Furthermore, WT–AAV–PREP showed significantly higher insulin levels at time 15 compared with WT–AAV–EGFP and *Prep*$^{gt/gt}$–AAV–PREP (Fig. 4*I*). Glucagon levels at time 0 were significantly higher in *Prep*$^{gt/gt}$ mice infected with AAV–EGFP compared with all other groups (Fig. 4*J*).

Discussion

The present study reveals an unexpected role of prolyl endopeptidase in glucose homeostasis. We have shown that Prep is expressed in the VMH. Prep knockdown mice (*Prep*$^{gt/gt}$) showed a significant reduction of glucose-induced neuronal activation in the VMH together with glucose intolerance but normal insulin sensitivity. *Prep*$^{gt/gt}$ mice showed reduced fasting insulin and increased fasting glucagon levels together with an impaired in vivo glucose-induced insulin secretion. Analyses of islets morphology showed no difference between *Prep*$^{gt/gt}$ and WT mice, and in vitro islet function was similar between the two groups, indicating that the reduced pancreatic PREP expression in *Prep*$^{gt/gt}$ mice may not be the cause of the altered in vivo pancreatic function. *Prep*$^{gt/gt}$ mice showed increased sympathetic tone, and treatment of *Prep*$^{gt/gt}$ mice with a sympathetic nervous system antagonist significantly improved their glucose intolerance to a level similar to that of WT controls. In addition, WT mice centrally infused with a specific PREP inhibitor, S17092 (15), showed reduced glucose tolerance compared with vehicle infused mice, with a concomitant decrease in circulating insulin levels, suggesting that central PREP may play a role in the regulation of glucose metabolism and pancreatic secretion. In support of this, re-expression of PREP in the VMH of *Prep*$^{gt/gt}$ mice normalized glucose, insulin, and glucagon levels.

Although reported for the first time in 1971 (16), a physiological role of PREP as a cleaving enzyme until now remained elusive (17). Previous in vitro studies have indicated that PREP functions to inactivate short peptides with internal Pro-Xaa bound (8). However, several in vivo studies could not confirm these findings (8). Other putative functions have been hypothesized (18–21). Due to the lack of any transmembrane region or a lipid anchor domain (1) in PREP's sequence, these functions include participation in the inositol phosphate signaling (18, 19), protein secretion, and/or axonal transport (20) and protein–protein interaction (21).

Our study unmasked a functional role for PREP in glucose metabolism in vivo. PREP expression in the VMH together with a decreased glucose-induced neuronal activation in the VMH, an impaired glucose tolerance, and glucose-induced pancreatic secretion in *Prep*$^{gt/gt}$ mice suggest a novel function of PREP in the hypothalamic regulation of glucose and pancreatic functions. Our data show that PREP affects circulating insulin and glucagon levels but not their sensitivity in peripheral tissues. In support of this, although at baseline condition *Prep*$^{gt/gt}$ mice showed significantly greater hepatic glucose production (HGP),

PHYSIOLOGY

hyperinsulemia significantly suppressed HGP in *Prep*$^{gt/gt}$ mice, indicating that hepatic insulin sensitivity is not affected in these mice. Because both fasting insulin and glucagon levels and glucose-induced insulin secretion were affected in *Prep*$^{gt/gt}$ mice, we investigated pancreas morphology and function. Histological analysis of the pancreas revealed no differences between *Prep*$^{gt/gt}$ and WT mice. Moreover, perifusion experiments of isolated pancreatic islets showed no difference in GSIS. These data were further supported by the experiment in which acute central inhibition of PREP activity increases circulating glucose and decreases insulin levels. Finally, the effect of PREP re-expression selectively in the VMH of *Prep*$^{gt/gt}$ mice argues that central PREP action plays an important role in glucose-induced insulin secretion.

The mechanism by which hypothalamic PREP controls glucose-induced insulin secretion may involve the ANS. Indeed, we found that the sympathetic tone of *Prep*$^{gt/gt}$ mice was increased compared with their WT controls as shown by the increased norepinephrine levels in the pancreas of fasted *Prep*$^{gt/gt}$ mice compared with fasted WT controls. Furthermore, when *Prep*$^{gt/gt}$ mice were treated with a β-adrenergic receptor antagonist, propranolol, at a dose that did not affect the GTT of WT mice, a significant improvement in glucose tolerance was observed in *Prep*$^{gt/gt}$ mice, showing now a glycemic profile similar to that of WT controls. The VMH has been shown to directly project to a number of autonomic centers in the brainstem regions, including the rostral ventrolateral medulla, a primary regulator of the sympathetic nervous system projecting into the sympathetic preganglionic neurons in the spinal cord (22). Furthermore, by projecting into other hypothalamic and extrahypothalamic areas, VMH neurons may also indirectly influence sympathetic activities (23) to regulate glucose homeostasis.

Because both parasympathetic and sympathetic nervous systems contribute significantly to the insulin and glucagon secretory responses (24, 25), it is conceivable that central PREP, via direct or indirect projections to the ANS, may affect pancreatic function. In support of our study, two recent reports (11, 26) showed that hypothalamic glucose sensors play an important role in the control of insulin secretion (26) and that specific reduction of insulin receptor levels in the VMH produces glucose intolerance and islet dysfunction (11). Similar to this latter work, we found that *Prep*$^{gt/gt}$ mice have impaired glucose sensing and activation of insulin receptors in the VMH. Finally, re-expression of PREP in the VMH of *Prep*$^{gt/gt}$ mice normalized glucose sensitivity and insulin and glucagon secretion.

In summary, our study shows that central Prep plays an important role in the regulation of glucose sensing and insulin and glucagon secretion. Future studies are warranted to define the mechanism(s) of action of central PREP in the regulation of glucose sensing and pancreatic function.

Experimental Procedures

Animal Care. All animal care and experimental procedures were approved by the Yale University Institutional Animal Care and Use Committee. All mice were housed in a temperature-controlled environment (25 °C) with a 12-hr light and a 12-hr dark photoperiod. All animals (age 4–6 mo) were provided regular chow diet and water ad libitum unless otherwise stated.

Generation of Gene-Trap PREP (*Prep*$^{gt/gt}$) Mice. BayGenomics clone RRM213 (Mutant Mouse Regional Resource Centers, www.mmrrc.org) was identified as having an insertion in the second intron of the PREP gene in a 129-strain ES cell (9). As protein coding begins in the first exon, the resulting protein in the gene-trap mice would include the first 40 amino acids of this 710-residue protein before the inserted β-galactosidase, as previously reported (9). Founder chimeric mice were bred to B6 for at least 10 generations.

Metabolic Measurements. Adult male mice for *Prep*$^{gt/gt}$ and WT were acclimated in metabolic chambers (TSE System) for 4 d before the start of the recordings as previously published (27, 28). For body composition, adult males were scanned in an EchoMRI machine (Echo Medical Systems), and their body composition was calculated according to body weight.

Glucose, Insulin, and PTTs. Glucose tolerance tests were performed in 16-h fasted animals as previously reported (27, 28). Each animal received an i.p. injection of 2 g/kg body weight (BW) glucose (DeltaSelect) in sterile saline. Blood glucose and insulin levels were measured after 15, 30, 60, and 120 min. An ITT was performed in ad-libitum-fed mice (27, 28). Each animal received an i.p. injection of 1 U/kg of insulin (Actrapid, Novo Nordisk). A PTT was performed in 16-h fasted animals. Animals received an i.p. injection of 2 g/kg BW sodium pyruvate (Sigma-Aldrich, catalog #P5280).

In Situ Hybridization. In situ hybridization was based on our previously published protocol (27, 28). A 500-bp sequence between 1531 and 2030 was selected from the mouse PREP (GenBank accession no. NM_011156), synthesized (Biomatik), incorporated into pBluescript vector, and used as template (27, 28). ^{35}S-labeled riboprobes were then purified using sephadex columns (ProbeQuant G-50 Micro Columns, Pharmacia Biotech) following the manufacturer's protocol, and 5×10^5 cpm per section was used for the hybridization (27, 28).

X-Gal Staining. *Prep*$^{gt/gt}$ male mice were perfused with 4% paraformaldehyde. Brains were sectioned (50 μm), washed in PBS, and incubated overnight at 37 °C in the staining solution containing 25 mM $K_3Fe(CN)_6$, 25 mM $K_4Fe(CN)_6$3H2O, 2 mM $MgCl_2$ in PBS, and 1 mg/mL of X-Gal.

Real-Time RT-PCR. Real-time RT-PCR was performed as previously described (29) using the LightCycler 480 (Roche) and Taqman Gene Expression Assay primers (Applied Biosystems) in a 10-μL reaction volume in triplicates. All Taqman Gene Expression Assay primers used in our study are commercially available at Applied Biosystems (Prep: Mm 00448377_m1; Pck1: Mm01247059_g1; G6Pase: Mm00839363_m1; Ucp1: Mm00494069_m1; Gapdh: Mm99999915_g1; 18S: Mm03928990_g1).

Histological Analysis. Pancreas from WT and *Prep*$^{gt/gt}$ mice were collected and fixed in 4% (wt/vol) paraformaldehyde, in phosphate buffer 0.1 M, pH = 7.4. Five-μm sections were cut following routine paraffin processing and stained with hematoxylin and eosin. Duplicate nonstained sections were used for immunohistochemical detection of insulin and glucagon in pancreas.

c-fos Staining. Fasted WT and *Prep*$^{gt/gt}$ mice were injected i.p. with 2 g/kg glucose (DeltaSelect) in sterile saline. Mice were then perfused for 30 min, and c-fos staining was performed according to our previously published protocol (29).

Western Blot Analysis. VMH and hypothalamus samples were collected from mice that were fed, overnight-fasted, or fasted and injected with saline, glucose (2 g/kg BW), or insulin (0.75 U/kg BW; Actrapid; Novo Nordisk) and killed 5 or 30 min after the injection. Protein lysates from all of the tissues from WT and *Prep*$^{gt/gt}$ mice were prepared as previously described (30). Membranes were incubated overnight with anti-insulin receptor (Cell Signaling, catalog #3025) and antiphospho insulin receptor (Invitrogen, catalog #44800G). Membranes were reused to detect β-actin (Sigma, catalog #A5441).

Hyperinsulinemic-Euglycemic Clamp. Hyperinsulemic-euglycemic clamp studies were performed as previously reported (11). Insulin infusion rate was 2.5 mU·kg^{-1}·min^{-1}, and a variable-rate glucose infusion was used to maintain plasma glucose levels between 120 and 130 mg/dL for 120 min. Blood samples were collected at regular intervals for measurement of plasma glucose, hormones, and tracer. Red blood cells collected from a donor animal and resuspended in heparinized saline were constantly reinfused back into each animal to prevent volume depletion and anemia.

Pancreas and Islet Studies. Isolated islet studies were conducted as previously described (31). Islets were loaded into a perifusion chamber with acrylamide gel column beads (Bio-Gel P4G; Bio-Rad) and basal perfusion buffer (Krebs-Ringer buffer with 2.5 mmol/L glucose and 0.2% fatty acid-free BSA). After a 1.5-h equilibration period, islets were perifused and samples were collected at regular intervals. At the end of the perifusion, islet DNA was isolated and quantified for normalization of insulin data using a Picogreen dsDNA quantitation kit (Invitrogen) according to the manufacturer's instructions.

Pancreas NE Measurement. Each frozen pancreas was quickly weighed before it was sonicated in 0.1 M of cold perchloric acid containing dihydroxybenzylamine (DHBA) as internal standard. Following centrifugation at 30,000 × *g* for 15 min at 4 °C, the catechols in a portion of the supernatant were extracted on alumina at pH 8.6, washed with water, and eluted in 0.1 M

of perchloric acid (32). NE and DHBA were separated in a reverse-phase HPLC column and detected electrochemically. The ratio of NE and DHBA peak heights was calculated in each sample, and the NE concentration was quantified in relation to external standards of NE and DHBA and expressed as nanogram/milligram of tissue weight.

Propranolol Treatment. Propranolol (Sigma; nonselective β1 and -2 blocker) was administrated to *Prep*$^{gt/gt}$ mice i.p. for 3 d at a dose of 10 μg/g BW (33). A group of *Prep*$^{gt/gt}$ mice were used as controls and injected with an equal volume of saline. All *Prep*$^{gt/gt}$ mice were fasted overnight, and propranolol was last injected 2 h before the GTT was performed. After determination of fasted blood glucose levels using a glucometer (Lifescan), mice were injected with 2 g/kg glucose (DeltaSelect) in sterile saline. Blood glucose levels were measured.

S17092 Treatment. WT mice were i.c.v. cannulated 1 wk before the i.c.v. infusion of S17092 (15). After overnight fasting, all mice were infused for 30 min with either S17092 (10 μM in saline containing 0.5% DMSO at a rate of 0.1 μL/min; Sigma catalog #SML0181) or the equivalent volume of vehicle. After determination of blood glucose levels, 2 g/kg glucose (DeltaSelect) in sterile saline was injected, and glucose and insulin levels were measured as described above.

Hormonal Measurements. Insulin (EMD Millipore, catalog #EZRMI-13K), glucagon (R&D Systems, catalog #DGCG0), and free T4 and T3 (Leinco Technologies, catalog #T182 and T183, respectively) levels were measured by ELISA according to the manufacturer's protocol.

AAV Plasmid Construction. Flag (DYKDDDDK)-tagged GFP was chosen as a control in the studies. The Flag-GFP fragment was digested from its original pENTR plasmid (from NIDA) and cloned into a pAAV expression vector carrying EF1α promoter (AAV–GFP). To generate AAV–PREP, cDNA encoding mouse prolyl endopeptidase (Origene, catalog #MC200777) was cloned into an AAV expression vector carrying EF1α promoter. PCR amplicon of the mouse PREP ORF was inserted into the backbone vector (AAV–GFP) using infusion reaction and the manufacturer's instructions (In-Phusion HD Cloning Kit, Clontech). Plasmids were transformed into Stbl3 cells (Invitrogen). Positive clones from each constructed plasmid were verified using PCR, purified plasmids were sequenced, and Flag tag was detected to confirm the protein expression of AAV–GFP and AAV–PREP.

Purification of AAV. Viral production was accomplished using a triple-transfection, helper-free method and purified as described (34). The virus was purified via iodixanol gradients as described (34) and titered using quantitative PCR.

AAV Injection into the VMH. AAV vectors expressing EGFP and PREP (~1×10^{11} viral particles/mL) were injected bilaterally into the VMH of anesthetized mice (coordinates, bregma: anterior–posterior, −1.3 mm; lateral, ±0.4 mm; dorsal–ventral, −5.8 mm) at a rate of 40 nL/min for 15 min. GTT was performed 2 wk post viral injection as described above. Blood samples were collected at different times to measure insulin and glucagon levels. Immunofluorescence staining and Western blot were performed to confirm the injection site and expression of EGFP and PREP using anti-Flag antibody (Sigma, catalog #F1804) and anti-PREP antibody (Abcam, catalog #ab58988).

Statistical Analysis. Two-way ANOVA was used to determine the effect of the genotype and treatment with the Prism 4.0 software (GraphPad Software). For repeated measures analysis, ANOVA was used when values over different times were analyzed. Significant effects were evaluated with Fisher's protected least significant difference post hoc test with Bonferroni's correction. When only two groups were analyzed, statistical significance was determined by an unpaired Student *t* test. A value of $P < 0.05$ was considered statistically significant. All data are shown as mean ± SEM unless stated otherwise.

ACKNOWLEDGMENTS. We thank the Yale Diabetes Research Center for partially supporting the clamp studies (Grant P30 DK-45735). This work was supported by National Institutes of Health Grants DK084065 and DK097566 (to S.D.) and by American Diabetes Association Research Award 7-11-BS-33 (to S.D.).

1. Venäläinen JI, Juvonen RO, Männistö PT (2004) Evolutionary relationships of the prolyl oligopeptidase family enzymes. *Eur J Biochem* 271(13):2705–2715.
2. Myöhänen TT, Venäläinen JI, García-Horsman JA, Piltonen M, Männistö PT (2008) Distribution of prolyl oligopeptidase in the mouse whole-body sections and peripheral tissues. *Histochem Cell Biol* 130(5):993–1003.
3. Dauch P, Masuo Y, Vincent JP, Checler F (1993) A survey of the cerebral regionalization and ontogeny of eight exo- and endopeptidases in murines. *Peptides* 14(3):593–599.
4. Agirregoitia N, Irazusta A, Ruiz F, Irazusta J, Gil J (2003) Ontogeny of soluble and particulate prolyl endopeptidase activity in several areas of the rat brain and in the pituitary gland. *Dev Neurosci* 25(5):316–323.
5. Bellemère G, Vaudry H, Mounien L, Boutelet I, Jégou S (2004) Localization of the mRNA encoding prolyl endopeptidase in the rat brain and pituitary. *J Comp Neurol* 471(2):128–143.
6. D'Agostino G, et al. (2013) Prolyl endopeptidase-deficient mice have reduced synaptic spine density in the CA1 region of the hippocampus, impaired LTP, and spatial learning and memory. *Cereb Cortex* 23(8):2007–2014.
7. Brandt I, Scharpé S, Lambeir AM (2007) Suggested functions for prolyl oligopeptidase: A puzzling paradox. *Clin Chim Acta* 377(1-2):50–61.
8. García-Horsman JA, Männistö PT, Venäläinen JI (2007) On the role of prolyl oligopeptidase in health and disease. *Neuropeptides* 41(1):1–24.
9. Perroud B, et al. (2009) In vivo multiplex quantitative analysis of 3 forms of alpha melanocyte stimulating hormone in pituitary of prolyl endopeptidase deficient mice. *Mol Brain* 2:14.
10. Fioramonti X, Song Z, Vazirani RP, Beuve A, Routh VH (2011) Hypothalamic nitric oxide in hypoglycemia detection and counterregulation: A two-edged sword. *Antioxid Redox Signal* 14(3):505–517.
11. Paranjape SA, et al. (2011) Chronic reduction of insulin receptors in the ventromedial hypothalamus produces glucose intolerance and islet dysfunction in the absence of weight gain. *Am J Physiol Endocrinol Metab* 301(5):E978–E983.
12. Thorens B (2011) Brain glucose sensing and neural regulation of insulin and glucagon secretion. *Diabetes Obes Metab* 13(Suppl 1):82–88.
13. Silva JE (1995) Thyroid hormone control of thermogenesis and energy balance. *Thyroid* 5(6):481–492.
14. Enerbäck S, et al. (1997) Mice lacking mitochondrial uncoupling protein are cold-sensitive but not obese. *Nature* 387(6628):90–94.
15. Barelli H, et al. (1999) S 17092-1, a highly potent, specific and cell permeant inhibitor of human proline endopeptidase. *Biochem Biophys Res Commun* 257(3):657–661.
16. Walter R, Shlank H, Glass JD, Schwartz IL, Kerenyi TD (1971) Leucylglycinamide released from oxytocin by human uterine enzyme. *Science* 173(3999):827–829.
17. Myöhänen TT, García-Horsman JA, Tenorio-Laranga J, Männistö PT (2009) Issues about the physiological functions of prolyl oligopeptidase based on its discordant spatial association with substrates and inconsistencies among mRNA, protein levels, and enzymatic activity. *J Histochem Cytochem* 57(9):831–848.
18. Schulz I, et al. (2002) Modulation of inositol 1,4,5-triphosphate concentration by prolyl endopeptidase inhibition. *Eur J Biochem* 269(23):5813–5820.
19. Williams RS, Eames M, Ryves WJ, Viggars J, Harwood AJ (1999) Loss of a prolyl oligopeptidase confers resistance to lithium by elevation of inositol (1,4,5) trisphosphate. *EMBO J* 18(10):2734–2745.
20. Schulz I, et al. (2005) Subcellular localization suggests novel functions for prolyl endopeptidase in protein secretion. *J Neurochem* 94(4):970–979.
21. Di Daniel E, et al. (2009) Prolyl oligopeptidase binds to GAP-43 and functions without its peptidase activity. *Mol Cell Neurosci* 41(3):373–382.
22. Lindberg D, Chen P, Li C (2013) Conditional viral tracing reveals that steroidogenic factor 1-positive neurons of the dorsomedial subdivision of the ventromedial hypothalamus project to autonomic centers of the hypothalamus and hindbrain. *J Comp Neurol* 521(14):3167–3190.
23. Zhang YH, Lu J, Elmquist JK, Saper CB (2000) Lipopolysaccharide activates specific populations of hypothalamic and brainstem neurons that project to the spinal cord. *J Neurosci* 20(17):6578–6586.
24. D'Alessio DA, Kieffer TJ, Taborsky GJ, Jr, Havel PJ (2001) Activation of the parasympathetic nervous system is necessary for normal meal-induced insulin secretion in rhesus macaques. *J Clin Endocrinol Metab* 86(3):1253–1259.
25. Kiba T (2004) Relationships between the autonomic nervous system and the pancreas including regulation of regeneration and apoptosis: Recent developments. *Pancreas* 29(2):e51–e58.
26. Osundiji MA, et al. (2012) Brain glucose sensors play a significant role in the regulation of pancreatic glucose-stimulated insulin secretion. *Diabetes* 61(2):321–328.
27. Jeong JK, Szabo G, Kelly K, Diano S (2012) Prolyl carboxypeptidase regulates energy expenditure and the thyroid axis. *Endocrinology* 153(2):683–689.
28. Jeong JK, Szabo G, Raso GM, Meli R, Diano S (2012) Deletion of prolyl carboxypeptidase attenuates the metabolic effects of diet-induced obesity. *Am J Physiol Endocrinol Metab* 302(12):E1502–E1510.
29. Diano S, et al. (2011) Peroxisome proliferation-associated control of reactive oxygen species sets melanocortin tone and feeding in diet-induced obesity. *Nat Med* 17(9):1121–1127.
30. Kwon Jeong J, Dae Kim J, Diano S (2013) Ghrelin regulates hypothalamic prolyl carboxypeptidase expression in mice. *Mol Metab* 2(1):23–30.
31. Jurczak MJ, et al. (2011) SGLT2 deletion improves glucose homeostasis and preserves pancreatic beta-cell function. *Diabetes* 60(3):890–898.
32. Morrow BA, Roth RH, Redmond DE, Elsworth JD (2011) Impact of methamphetamine on dopamine neurons in primates is dependent on age: Implications for development of Parkinson's disease. *Neuroscience* 189:277–285.
33. Commins SP, Watson PM, Levin N, Beiler RJ, Gettys TW (2000) Central leptin regulates the UCP1 and ob genes in brown and white adipose tissue via different beta-adrenoceptor subtypes. *J Biol Chem* 275(42):33059–33067.
34. Hommel JD, et al. (2006) Leptin receptor signaling in midbrain dopamine neurons regulates feeding. *Neuron* 51(6):801–810.